International Journal of Technology

http://ijtech.eng.ui.ac.id

Research Article

Modeling Equivalent Circulating Density During Drilling Operations in the Gulf of Thailand

Kanogkan Leerojanaprapa[1], Sudarat Suttaloon[2], Komn Bhundarak[3], Kittiwat Sirikasemsuk[4*]

[1]Department of Statistics, School of Science, King Mongkut's Institute of Technology Ladkrabang, Bangkok, 10520, Thailand

[2]KMITL Digital Analytics and Intelligence Center, School of Science, King Mongkut's Institute of Technology Ladkrabang, Bangkok, 10520, Thailand

[3]Department of Operations Management, Thammasat Business School, Thammasat University, Bangkok, 10200, Thailand

[4]Department of Industrial Engineering, School of Engineering, King Mongkut's Institute of Technology Ladkrabang, Bangkok, 10520, Thailand

[*]Corresponding author: kittiwat.si@kmitl.ac.th; Tel.: +66-2-329-8301 ext. 225; Fax: +66-2-329-8302

Abstract: Equivalent Circulating Density (ECD) represents the total hydrostatic pressure generated by drilling fluid while in motion. This prevents the internal pressure within the well from exceeding the fracture resistance of the rock, which could lead to lost circulation and an inability to effectively control the wellbore pressure. This research aims to predict ECD in 6.125-inch production section in Gulf of Thailand field by using five machine learning algorithms were utilized, namely Support Vector Machine (SVM), Random Forest (RF), Artificial Neural Networks (ANN), Gradient Boosting (GB), and Extreme Gradient Boosting (XGBoost). Various sensors from the Measure While Drilling (MWD), Logging While Drilling (LWD), and Pressure While Drilling (PWD) tools were used to collect raw data, totaling 38,863 records and 24 variables to predict the ECD value. The dataset was randomly split into 80% for training and validation and 20% for testing. The results indicate that the RF technique outperformed the other models in predicting ECD values, producing the lowest RMSE of 0.031. Therefore, the RF model is most suitable for further development and real-time application in predicting ECD values.

Keywords: Drilling operations; Equivalent circulating density; Machine learning models; Wellbore pressure

1. Introduction

Excavating and drilling for oil exploration and production is an inherently challenging and critically important task. Each drilling operation requires significant time and capital, making it a high-risk investment. Beyond the financial and time investments, drilling operations also entail navigating exceptionally high levels of risk. This passage highlights the challenges of drilling for oil and gas, particularly the risks associated with drilling to depths averaging 3-4 kilometers underground. The time and financial investments required for drilling are emphasized, with estimates ranging from 5 to 7 days and $600,000 to $800,000 per day or $4-6 million per well, depending on the depth (Amado, 2013; Hadi, 2023). This is considered a high-risk, high-cost investment.

The Equivalent Circulating Density (ECD) refers to the total hydrostatic pressure of the drilling mud under dynamic flow conditions. It represents the pressure loss that occurs in the annular space between the drill string and the wellbore wall due to mud circulation (Mitchell and Miska, 2011). ECD is considered one of the most critical parameters in both

https://doi.org/10.14716/ijtech.v17i2.7897
Received June 2025; Revised October 2025; Accepted January 2026

the design of drilling programs and the real-time monitoring of drilling operations. It plays a key role in maintaining wellbore stability and ensuring pressure balance within the borehole. It is essential to determine the appropriate pressure limits for the drilling system, especially the maximum allowable pressure that the formation can withstand without fracturing—referred to as the fracturing pressure. This is the key to preventing and reducing the likelihood of problems inside the well during the drilling process (International Association of Oil & Gas Producers, 2023). This threshold is typically established through leak-off tests (LOT) or formation integrity tests (FIT) and defines, the upper limit for acceptable ECD values during subsequent drilling phases. During drilling operations, the ECD serves as a control parameter for managing various variables to maintain the wellbore equilibrium. If the formation fractures due to excessive ECD, the drilling mud may be lost into the fractured formation, leading to a loss of circulation (Gamal et al., 2021a), which poses significant operational and safety risks.

However, the use of ECD measurement instruments requires special equipment such as Pressure While Drilling (PWD), in addition to the standard tools such as Measure While Drilling (MWD) and Logging While Drilling (LWD), instruments which are commonly used in the oil and gas industry. In addition, the cost of running the service is quite high, and the price also depends on fluctuations in oil and gas prices and limited in their use because they pose a high risk of equipment damage or failure to measure data during drilling operations in high temperature and high-pressure environments. In addition, traditional ECD estimation methods rely on downhole sensors, which are costly and limited the accuracy of purely physics-based models or complex mathematical models (Gamal et al., 2021a; Dabiri et al., 2025).

Furthermore, conventional hydraulic models often rely on simplified assumptions that may not fully capture the drilling operations' complex and dynamic nature. Therefore, accurate estimation of ECD is essential for maintaining wellbore stability and minimizing drilling risks. Machine learning approaches can model nonlinear relationships among drilling parameters and provide rapid estimation suitable for real-time applications. Therefore, studying machine learning–based ECD estimation can improvetherefore contributes to improved operational decision-making, reducereduced drilling risk, and enhanceenhanced efficiency, particularly in offshore environments with narrow operational margins, such such as the Gulf of Thailand. Therefore, the development of a robust real-time model using an appropriate machine learning approach is essential as a prototype for implementation as a decision-support tool to estimate the equivalent circulating density during drilling operations based on surface and downhole measurements.

Recently, studies have explored the application of machine learning and artificial intelligence techniques within the gas industry, including failure prediction (Noorsaman et al., 2023) or petroleum operations (Bahaloo et al., 2023) with ECD prediction based on drilling and mud parameters (Gamal et al., 2021a; Okonkwo and Joel, 2023) but the influence of real-time drilling parameters has not been explicitly addressed. Ahmadi et al., 2016 and Ahmadi, 2016 applied Least Squares Support Vector Machine (LSSVM), Adaptive Network-Based Fuzzy Inference System (ANFIS), and an enhanced Particle-Swarm Optimization technique combined with ANFIS (PSO-ANFIS) to predict ECD using a dataset of 644 records, relying solely on mud pressure, temperature, and initial density. The findings indicated that the SVM model achieved the best performance. In a subsequent study, Ahmadi et al., 2016 and Ahmadi, 2016 used the same dataset to predict ECD based on initial mud properties, utilizing PSO-ANN, Fuzzy Inference System (FIS), and a hybrid Genetic Algorithm-FIS (GA-FIS) approach. Their results showed that the PSO-ANN model outperformed the other techniques in terms of the coefficient of determination (R^2) and mean absolute percentage error (MAPE) between the actual and predicted ECD values. Additionally, H. Alkinani et al., 2019 developed an Artificial Neural Network (ANN) model with a single hidden layer comprising 12 neurons to estimate the Equivalent Circulating Density (ECD). The model utilized 7 input parameters, including pump rate, mud density, plastic viscosity, yield point, total flow area (TFA) of bit nozzles, drill pipe rotational speed (RPM), and weight on bit (WOB). Those 7 input variables were chosen based on the statistical and sensitivity analyses performed by Al-Hameedi et al., 2017 and experts'

opinions. The testing results demonstrated a high coefficient of determination (R^2) of 0.982. In the same year, Abdelgawad et al., 2019 developed ECD prediction models using both ANN and ANFIS approaches. Their ANN model utilized a single hidden layer with 20 neurons, while the ANFIS model employed five Gaussian membership functions for surface parameters, such as the rate of penetration (ROP), the weight of the mud flowing to the hole (MW), and the drill pipe pressure (DPP), without downhole measurements, and a linear function for outputs. Both models showed comparable accuracy in predicting ECD. Meanwhile, Rahmati and Tatar, 2019 developed an ECD prediction model using a Radial Basis Function (RBF) network, achieving excellent performance with an R^2 of 0.98 and an Average Absolute Percentage Error (AAP) of 0.22. The model was constructed using physical properties data covering a wide range of pressure and temperature for different drilling fluid types. Recently, Okonkwo and Joel, 2023 developed an Artificial Neural Network (ANN) model to predict ECD in high-pressure, high-temperature (HPHT) wells. The model used field data to train the network with 11 physical input variables. The optimized model achieved a high prediction accuracy with R^2 of 0.9993, and outperformed existing ECD models. It can be observed that most existing models are built using static input data derived mainly from physical parameters.

Studies related to the utilization of real-time data for developing AI-based predictive models are summarized as follows. Abdelaal et al., 2023 addressed critical well-control challenges, such as fluid loss, formation fracturing, kicks, and blowouts. In this study, a Random Forest (RF) model was developed using real-time drilling hydraulic parameters—such as initial mud weight, standpipe pressure, and pump rate—to accurately predict Equivalent Circulating Density (ECD). A total of 5,140 data points were used to develop a comprehensive data analytics framework, which contributed to substantial improvements in predictive accuracy. The model achieved high performance, with a correlation coefficient (R) of 0.99. Recently, Alsaihati et al., 2021 created predictive models for ECD using seven key drilling parameters, such as mud pump rate, rate of penetration (ROP), drill string rotation speed (RPM), standpipe pressure (SPP), WOB, and drilling torque. They used SVM, RF, and Functional Network (FN) algorithms. The dataset was gathered from two horizontal wells (5-7/8 inches in diameter). Their models achieved high predictive accuracy with R^2 values ranging from 0.95 to 0.99 and Root Mean Squared Errors (RMSE) between 0.23 and 0.42. Gamal et al., 2021b proposed to apply the ANN model with mechanical drilling parameters from surface rig sensors to cope with real-time ECD prediction, achieving R of 0.98 and average absolute percentage error (AAPE) 0.3%. Lastly, Roy et al., 2022 showcased the application of XGBoost, RF, SVM, Decision Tree, and Elastic Net Regression for predicting ECD during drilling, highlighting its significance in mitigating risks of fluid loss and well kicks. Using drilling data from a Texas oil well, a dataset of over 16,000 points was prepared through scaling and Principal Component Analysis (PCA). RF emerged as the most accurate model with an R^2 of 0.992, followed by SVM with an R^2 of 0.987.

A critical review of the existing literature demonstrates that models have significantly enhanced ECD prediction performance (as shown in Table 1). However, methodologies for ECD prediction vary considerably, particularly in terms of the nature of datasets used for model training. A common limitation identified across numerous studies is the restricted number of independent variables—most models predominantly relied on downhole pressure and temperature. This reliance poses challenges, especially when such measurements are difficult to obtain in real time from logging while drilling. This study proposes a machine learning-based predictive model that enhances the accuracy of ECD estimation under dynamic drilling conditions by utilizing real-time sensor data acquired during oil and gas well drilling operations.

Table 1 Critical review of ECD prediction by using ML algorithms in literature

Authors	Model	Independent variables														No. records
		Pressure	Temperature	Initial density	Flow rate	Mud weight	Total flow area	Rev. per min.	Yield point	Plastic viscosity	Rate of penetration	Weight on bit	Torque	Hook load	Mud pumping rate	Depth	
Ahmadi et al., 2016	LSSVM ANFIS PSO-ANFIS	✓	✓	✓													NA
Ahmadi, 2016	PSO-ANN FIS GA-FIS	✓	✓	✓													644
H. Alkinani et al., 2019	ANN				✓	✓	✓	✓	✓	✓		✓					2,000
Abdelgawad et al., 2019	ANFIS ANN	✓				✓					✓						2,376
Rahmati and Tatar, 2019	Radial Basis Function	✓	✓	✓													884
Alsaihati et al., 2021	SVM RF Functional Network	✓			✓			✓			✓	✓	✓	✓			3,567
Gamal et al., 2021b	ANN ANFIS	✓		✓				✓			✓	✓	✓		✓		4,700
Roy et al., 2022	XGBoost RF SVM Decision Tree Elastic Net				✓	✓						✓			✓		16,000
Abdelaal et al., 2023	RF	✓				✓									✓		5,140
Okonkwo and Joel, 2023[1]	ANN	✓	✓		✓	✓										✓	1,011

[1]Six variables are excluded from the table: average equivalent annular diameter across the BHA, average equivalent annular diameter across the DP, flow conduit length across the BHA, flow conduit length across drill pipe, average annular velocity across the BHA, and average annular velocity across drill pipe.

Several models have been proposed for the real-time prediction of Equivalent Circulating Density (ECD), including those by Gamal et al., 2021b, Alsaihati et al., 2021, and Roy et al., 2022. These studies demonstrate that machine learning algorithms can provide faster and more accurate predictions, enabling effective real-time monitoring, which is particularly critical for drilling operations within narrow operational windows. Accordingly, this study evaluates five machine learning algorithms—Support Vector Machine (SVM), Random Forest (RF), Gradient Boosting (GB), Extreme Gradient Boosting (XGBoost), and Artificial Neural Networks (ANN)—to identify the most suitable model for ECD prediction. These algorithms are well suited to handling nonlinear relationships, sensor noise, and real-time adaptability. The primary objective of this research is to compare the predictive performance of these five machine learning approaches for ECD estimation in the Gulf of Thailand using real-time data acquired from measurement and logging tools, specifically Measurement While Drilling (MWD) and Logging/Pressure While Drilling (LWD/PWD); in oil and gas production wells.

2. Methods

1. Equivalent Circulating Density (ECD)

The Equivalent Circulating Density (ECD) refers to the effective fluid density within the wellbore during circulation, accounting for both the hydrostatic pressure from the static mud column and the additional pressure losses due to fluid movement (Raabe and Jortner, 2021). The equation for calculating the density of the circulating mud or ECD is provided below:

$$\mathrm{ECD} = \mathrm{MW} + \frac{\mathrm{APL}}{0.052 \times \mathrm{TVD}} \tag{1}$$

when:

ECD = equivalent circulating density (ppg)
MW = static mud weight (ppg)
APL = annular pressure loss (psi)
TVD = True vertical depth (ft)

This equation accounts for the mud density and pressure loss, which is normalized by the hole depth.

2. Machine Learning Algorithms Considered

All predictor variables used in this research are continuous data with a linear relationship between variables as the borehole depth increases, which includes multiple independent variables and aims to predict ECD values. According to the defined property based on the dataset, algorithms in the machine learning regression model family are defined, and the results of the experiments are compared with these parameters presented in this research.

2.1 Support Vector Machine: SVM

Support Vector Machine (SVM) is a robust supervised machine learning algorithm primarily used for classification and regression models. In SVM regression, kernel functions are mathematical functions that enable the algorithm to optimize variable values in a polynomial manner without altering the initial variables' form and relationships. Linear kernels produce linear decision boundaries under the assumption that the relationship between the features and the target variable is linear. On the other hand, Non-linear kernels, such as polynomial or Radial Basis Function (RBF) kernels, allow to capture more complex decision boundaries (Sun et al., 2020). These shapes can be curves, circles, or more intricate shapes (Rahmati and Tatar, 2019).

It seeks the best graph or hyperplane in higher dimensions, covering the maximum number of data points (Awad and Khanna, 2015). This optimization involves utilizing different kernel functions to find the most suitable hyperplane. SVM is extended to solve regression problems, known as Support Vector Regression (SVR). SVR formulates function approximation as an optimization problem that aims to identify the flattest function within a defined margin (ϵ-tube) around the data while minimizing prediction errors outside this margin—differences between actual and predicted outputs—as low as possible.

The objective is to minimize the prediction error by ensuring that the estimated function closely approximates the actual output. The objective function of the optimization problem presented in Equation (2) is formulated, where C acts as a regularization parameter that helps balance the trade-off between minimizing flatness and reducing error in this multi-objective optimization. For example, increasing the value of C places more emphasis on minimizing the error and ξ_i^2 are slack variables to measure their deviation. However, to use a Kernel function, we must transform it into a dual-objective function. This constrained quadratic optimization problem can be solved by formulating the Lagrangian function and applying Lagrange multipliers:

$$\text{Minimize } \frac{||\omega||^2}{2} + C\sum_{i=1}^{N}\left(\xi_i^2 + \xi_i^*\right) \tag{2}$$

subject to

$$\begin{aligned} y_i - w^T x_i &\leq \varepsilon + \xi_i^* \\ w^T x_i - y_i &\leq \varepsilon + \xi_i \\ \xi_i^* &\geq 0 \end{aligned} \tag{3}$$

The minimum objective of the objective function in Equation (2) is found by solving the partial derivatives with respect to the variables and setting them to zero, in accordance with the Karush-Kuhn-Tucker (KKT) conditions. Therefore, the key hyperparameters of SVR include the regularization parameter (C), the epsilon-insensitive loss parameter (ε), and the kernel parameter (γ). These hyperparameters control the trade-off between model complexity and generalization, tolerance to prediction errors, and influence range of training samples.

2.2 Random Forest Regression: RF

Random Forest Regression employs a method of generating decision trees by randomly sampling both the sample data and variables. It then predicts variable values based on the ensemble structure generated from combining the results of each decision tree (Cutler et al., 2012). This ensemble approach yields highly accurate and stable predictive models. The RF effectively handles complex data and intricate relationships between output variables. Each tree splits nodes by evaluating a random subset of features, a technique that helps reduce correlation between trees. This process is part of the bootstrapping approach used in Random Forests (Hegde and Gray, 2017). Additionally, it can automatically manage abnormal data or missing values. Consequently, RF is capable of efficiently managing noise because of its inherent real-time adaptability. Random Forest is an ensemble learning method. The trees within the forest use an optimal split strategy, such as setting the splitter to ”best” in the DecisionTreeRegressor. The max samples parameter determines the size of each subset when bootstrap samples are made about one-third of the samples; otherwise, each tree is built using the entire dataset (Pedregosa et al., 2011).

2.3 Artificial Neural Networks: ANN

ANNs constitute a family of algorithms designed to identify complex relationships within a dataset by simulating the functionality of the human brain. These networks consist of multiple layers, including an input layer, at least one hidden layer, and an output layer. Each layer

contains neurons that process and transform input data. In an ANN, data are passed through the input layer, processed within the hidden layers, and the results are outputted.

The ANN architecture is characterized by the number of hidden layers, the number of neurons within each layer, and the activation functions applied to process the data. As shown-illustrated in Figure 1, the input layer receives the data, and each input is connected to every neuron in the subsequent hidden layers. This interconnected structure enables the ANN to learn complex patterns and relationships within the data (Gallo, 2015).

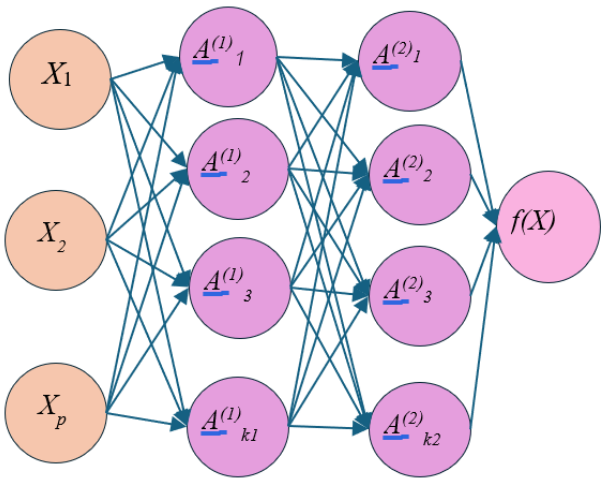

Figure 1 Neural network with a hidden double layer

$$f(X) = \beta_0 + \sum_{k=1}^{K} \beta_k h_k(X) \tag{4}$$

Each hidden layer comprises a specified number of neurons, each paired with an activation function. The activation function introduces nonlinearity between input and output (Ali, 1994). This process is constructed in two stages. First, the k hidden-layer activations $A_k (k = 1, 2, ..., K)$ are computed as nonlinear functions of the input features $X_1, X_2, ..., X_P$, given by:

$$A_k = h_k(X) = g\left(w_{k0} + \sum_{j=1}^{P} w_{kj} X_j\right) \tag{5}$$

where:

$g(z)$ is a predefined nonlinear activation function, and

w_{kj} are the input-to-hidden layer weights.

The network output is expressed as follows:

$$f(X) = \beta_0 + \sum_{k=1}^{K} \beta_k A_k \tag{6}$$

The parameters β_k and β_0 are optimized during training to minimize the prediction error.

The preferred choice in modern neural networks is the ReLU (rectified linear unit) activation function, which takes the following form:

$$g(z) = z_+ = \begin{cases} 0 & \text{if } z < 0 \\ z & \text{otherwise} \end{cases} \tag{7}$$

The fitting of a neural network involves estimating the unknown parameters in Equation (5). The squared-error loss function is commonly used for quantitative responses, with parameters

optimized to minimize this loss. Contemporary neural networks often consist of multiple hidden layers, each typically containing numerous units. Equation (8) represents the first hidden layer, with the corresponding Equation (9) being applied.

$$A_k^{(1)} = h_k^{(1)}(X) = g\left(w_{k0}^{(1)} + \sum_{j=1}^{P} w_{kj}^{(1)} X_j\right) \quad \text{for } k = 1, 2, 3, ..., K \tag{8}$$

The second hidden layer receives the activations $A_k^{(1)}$ from the first hidden layer as inputs and computes new activations for the subsequent layer for $l = 1, 2, 3, ..., K_l$.

$$A_l^{(2)} = h_l^{(2)}(X) = g\left(w_{l0}^{(2)} + \sum_{k=1}^{K} w_{lk}^{(2)} A_k^{(1)}\right) \quad \text{for } l = 1, 2, 3, ..., K_l \tag{9}$$

Note that each activation function in the second layer $A_l^{(2)} = h_l^{(2)}(X)$ is a function of the input vector X.

According to the additional superscript notations in Equations (8) and (9):

$w_{\ell k}^{(2)}$ is the weight connecting neuron k (layer 1) to neuron l (layer 2),

K_1 and K_2 are the number of neurons in the first and second hidden layers, respectively.

2.4 Gradient Boost Regression: GB

GB is indeed a technique within the ensemble methods such as Random Forest. It employs the principle of collectively learning from different decision trees, where each tree is constructed based on random samples of data and variables. Each tree predicts values based on its structure. However, the key difference lies in how GB adjusts the weights of each tree to fit the sample data. In GB, each successive tree is built to correct the errors from the previous trees by adjusting the weights of variables in the sample data. The new tree focuses on the remaining errors and predicts values accordingly. This process is repeated iteratively until the errors are significantly minimized (Goyal, 2021). This ability to iteratively adjust to the sample data makes GB highly effective in minimizing errors and improving predictive accuracy.

$$y_m = \arg\min \sum_{i=1}^{n} L(y_i; F_{m-1}(x_i)) + \gamma h_m(x_i) \tag{10}$$

where:

$F_{m-1}(x)$ is the previous model,

$h_m(x_i)$ is the decision tree made on the residuals,

where m is the number of DT. When m = 1 is defined as the 1^{st} DT, and when it is "M," it is defined as the last DT

γ_i is the predicted value that minimizes the loss function.

2.5 Extreme Gradient Boosting: XGBoost

XGBoost, or Extreme Gradient Boosting, is developed from the GB technique that emphasizes performance and speed of operation. It is a machine learning algorithm under ensemble learning and introduces additional features, such as weak learners as regularization and handling of missing values, to enhance predictive accuracy and efficiency. It can be used with any complex data and supports high-speed learning. XGBoost's capability to manage large datasets and operate swiftly makes it a valuable tool for accurate and efficient data analysis and prediction in various scenarios.

XGBoost is recognized for its efficiency in optimizing the loss function by leveraging Hessian information, which makes it more effective in training than GBM. It also incorporates regularization techniques, such as L1 and L2, to prevent overfitting, further boosting its performance. L1 regularization aims to reduce feature weights or coefficients to zero, effectively performing feature selection, while L2 regularization works to uniformly shrink the coefficients, helping to address multicollinearity. By incorporating both regularization techniques, XGBoost is better able to prevent overfitting compared to GBM. For simplicity, the squared loss function is selected to minimize the squared error. The modeling process begins with initializing the function $F_0(x)$, which serves as the initial prediction model. This function is chosen to minimize the loss function—in this case, the Mean Squared Error (MSE)—defined as:

$$F_0(x) = \arg\min \sum_{i=1}^{n} L(y_i, y) \tag{11}$$

$$\arg\min \sum L(y_i; y) = \arg\min \sum (y_i - y)^2 \tag{12}$$

The residuals from the initial prediction function $F_0(x)$ are used to train the first regression tree $k_1(x)$, which is an expression tree designed to reduce the residuals from the previous step by $F_0(x)$. This function is obtained by adding the output of $h(x)$ to the initial model $F_0(x)$, effectively allowing $h(x)$ to correct the residuals from the previous step. Within each regression tree, the leaf nodes estimate the average value of the residuals $(y - F_0(x))$. The boosting process continues iteratively, where each subsequent learner $k_m(x)$ is trained on the residuals of the preceding function $F_{m-1}(x)$. In this case, the procedure is repeated for two additional steps to construct $k_2(x)$ and $k_3(x)$, leading to increasingly accurate ensemble predictions.

2.6 Materials and Methods

This study presents the process of constructing the ECD predictive model, as shown in Figure 2. The process includes collecting data during data preparation, and cleaning data to improve data quality. Next, features are selected to provide input variables. All input features will be used to construct ML models to predict the ECD value by tuning all essential parameters for specific ML algorithms to optimize the model parameters along with the training dataset to train the model, which was subsequently validated using the testing dataset. If the model shows low performance, the model should be retrained to obtain the optimal parameters for predicting ECD.

1. **Data Collection**

   Gathering data during a production/reservoir section located in the Gulf of Thailand. Forty-six variables were collected over a one-year period from May 2022 to May 2023, and a total of 54,482 data records were collected. Furthermore, the various key variables utilized in this research have undergone preliminary selection and adjustments to align with the standardized data obtained from sensors for the MWD and LWD employed during the drilling operations. Therefore, the total of 46 selected variables are presented as Supplementary Material, Table S1. All input variables have undergone the variable selection process for fitting to the ECD model with the training dataset.

2. **Data Preparation**

   In variable selection, the first step is to eliminate duplicate data using the ”duplicated” function within the assisted learning tool. This is because the raw data used in this research is obtained from various sensors of the drilling equipment, which measure and record data at specified intervals. Therefore, duplicate data are collected at the same depth each time the drill string is pulled out and reinserted for further drilling. These redundant data entries contribute to biasing the model excessively toward this duplicated information, thus not accurately reflecting reality. After removing duplicate data, the

raw data collected for this research, totaling 78,592 entries, was reduced to 54,482 entries with 46 variables. These refined data entries are then used for the subsequent analysis. Subsequently, the missing data in each variable was assessed using the Missing Value function within the assisted learning tool. It was identified that 7 variables had missing data ranging from 60% to 95%, including TEMP_DNI.1, PEF, ROP5.1, PEB, NEAR, FAR, and DCAV. One variable, BIT_CONF, had missing data exceeding 7%. Further theoretical investigation revealed that these 8 variables were not directly or indirectly related to ECD values, as shown by Raabe and Jortner, 2021 and Saasen, 2013. To ensure the accuracy of the model, these 8 variables were consequently removed. This reduction resulted in 37 variables for the following analysis.

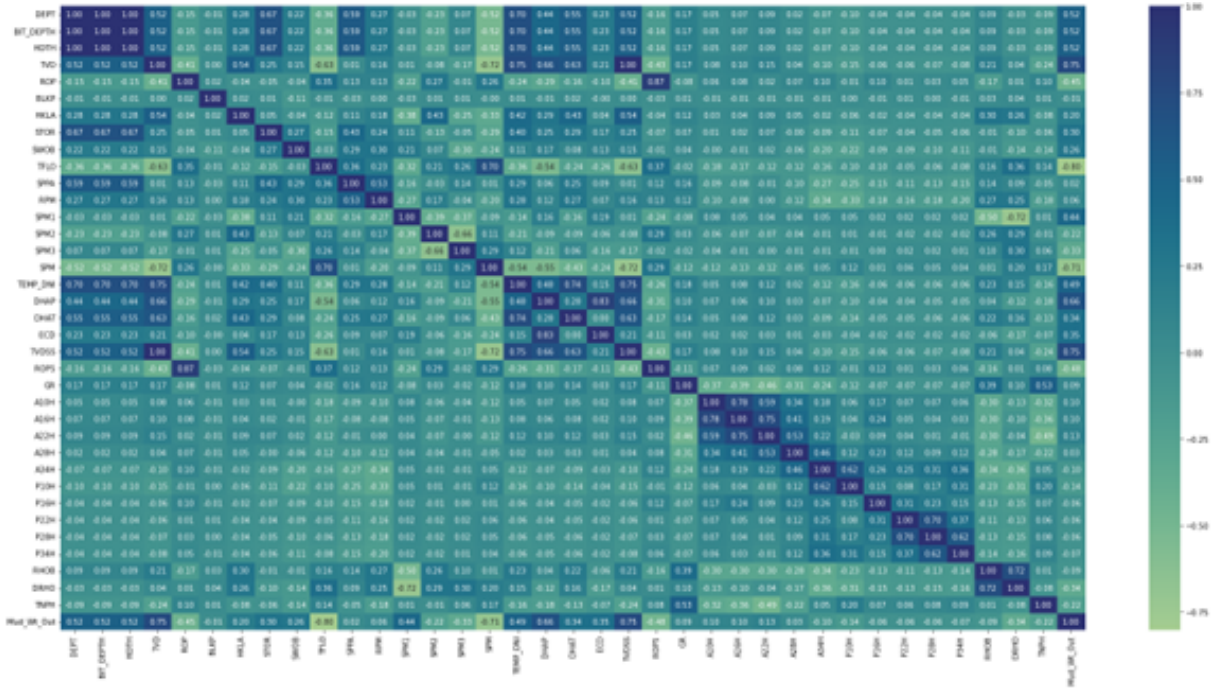

Figure 2 Correlation matrix of drilling parameters and ECD. The red square highlights a group of variables exhibiting strong intercorrelation among independent variables, while showing weak correlation with Equivalent Circulating Density (ECD)

The next step is the data validation process, which involves detecting, correcting, deleting, or replacing any missing or erroneous raw data once the data preparation is complete. The dataset that is prepared for use must closely align with reality to ensure the highest level of accuracy. This can be achieved by addressing abnormal data (errors) that typically arise from sensor malfunctions or data reading failures during drilling equipment operations. Drilling equipment often encounters malfunctions or failures, resulting in abnormal readings or consistent default values such as -999.25. These abnormal data are removed, such as geophysical data interpretation. This includes determining petrochemical types, rock layer porosity, water saturation, and other geological characteristics. The records in which these errors are detected according to the reasons above are removed from the entire dataset. Therefore, the full dataset was left with 48,579 entries and 37 variables for preprocessing and subsequent analysis.

According to feature selection, the correlation coefficient analysis of various variables using the Correlation Matrix, employing Seaborn's Heatmap function, as depicted in Figure 3, it is observed that variables representing lithological properties often exhibit significant correlations among themselves by exhibiting correlation coefficients ranging from 0.8 to 0.99, while excluding minimal correlation with the ECD, typically ranging from 0 to 0.02. These variables include A10H, A16H, A22H, A28H, and A34H.

Furthermore, P10H variables such as P10H, P16H, P22H, P28H, and P34H also demonstrate substantial interrelations, with maximum correlation coefficients reaching up to 0.7. Notably, variables ROP and ROP5, although of the same type, differ in that ROP represents the rate of penetration at the time of data collection, whereas ROP5 signifies the average rate of penetration over every 5-foot interval. Consequently, their correlation coefficient is notably high, up to 0.87. Additionally, concerning variables SPM, SPM1, SPM2, and SPM3, upon data exploration, it is evident that the sum of SPM1, SPM2, and SPM3 equals the variable SPM. To mitigate multicollinearity, the researcher opts to eliminate 12 variables, leaving 25 independent variables to be used in the subsequent stages of analysis and prediction of ECD values.

3. **Model Fitting**

Before constructing the ECD model, the dataset was randomly split into training and testing subsets using an 80:20 ratio, resulting in 38,863 and 9,716 records, respectively. The collected data represent a subset to represent regular drilling operations and are not influenced by time-oriented effects. The training set was used to train the model to learn underlying patterns, whereas the testing set was employed to evaluate the model's predictive performance on unseen data. In this study, 24 variables were selected as independent inputs, and ECD was designated as the dependent output variable. The 5 machine learning algorithms—SVM, RF, GB, XGBoost, and ANN—were employed to develop predictive models with the training dataset. To ensure that the models captured the key variations in ECD, the hyperparameters were optimized using GridSearchCV during the training phase. Multiple experiments were conducted to evaluate the model performance and identify the optimal configurations. During testing, the models with the best-tuned parameters were applied to previously unseen data to assess their generalization capability.

Finally, a model performance comparison was performed using a testing dataset to assess the accuracy of the models, including the root mean square error (RMSE), coefficient of determination (R^2), mean absolute error (MAE), and mean square error (MSE).

3. Results and Discussion

Descriptive statistical analysis of the 25 independent variables, as presented in Supplementary Material Table S2, indicates the absence of statistically abnormal values in the preprocessed dataset, which consists of 48,579 complete records. The analysis confirms that the input variables exhibit sufficient quality and variation to support the accurate prediction of ECD using machine learning techniques. Accordingly, the full dataset—comprising 24 independent variables and one dependent variable (ECD)—was used for modeling. The subsequent section presents the experimental results, including hyperparameter optimization and model performance comparisons.

3.1 Result of the experiments from the training data

A total of 38,863 records were used as the training dataset to construct models using five machine learning algorithms. In the experimental setup for predicting Equivalent Circulating Density (ECD) values, based on real-world data from the 6.125-inch drilling process in the Gulf of Thailand, all five machine learning models were evaluated using the GridSearchCV algorithm to optimize hyperparameters, with the specific parameter ranges outlined in Table 2. The best-performing parameters were selected to assess model accuracy on the testing dataset using the minimum values of Mean Squared Error (MSE) and Root Mean Squared Error (RMSE). Table 2 summarizes the final optimal parameters used to construct the predictive ECD models.

Table 2 Experimental setup of hyperparameter values for 5 algorithms in the experiments

Algorithm	Hyperparameter	Definition	Range of the parameters	Optimal
SVM	kernel	Kernel type	'linear', 'poly', 'rbf'	'linear'
	gamma	Kernel coefficient	'scale', 'auto'	'scale'
	C	Regularization parameter	1.0	1.0
RF	n_estimators	Number of estimators	50, 60, 70, 80, 90, 100, 150, 200	60
	min_samples_leaf	Minimum number of samples required at leaf node	1	1
	min_samples_split	Minimum number of samples required to split an internal node	2	2
ANN	hidden_layer_sizes	Number of hidden layers	1, 2, 3, 5, 15, 25, 35, 45	3
		Number of neurons per layer	3, 5, 15, 30, 45	45
	activation	Activation function for hidden layer	'identity','logistic', 'sigmoid' 'tanh', 'relu'	'sigmoid'
	max_iter	Maximum number of iterations	20, 200	20
	learning_rate_init	Initial learning rate used	0.001	0.001
GB	learning_rate	Learning rate shrinks the contribution of each tree	0.1	0.1
	min_samples_split	Minimum number of samples required to split an internal node	2	2
	max_depth	Maximum depth of individual regression estimators	3, 5, and 7	3
	n_estimators	Number of estimators	100, 200, 300, 400, and 500	100
	subsample	Fraction of samples used for fitting the individual base learners	1.0	1.0
XGBoost	learning_rate	Step size shrinkage used in the update to prevent overfitting	0.3	0.3
	gamma	Minimum loss reduction required to make a further partition on a tree leaf node	0	0
	max_depth	Maximum depth of a tree	4, 6, 8	6
	n_estimators	Number of boosting rounds (or trees) used in the ensemble	100, 200, 300, 400, and 500	400
	colsample_bylevel	Subsample ratio of columns when constructing each tree	1.0	1.0
	subsample	Subsample ratio of training instances	1.0	1.0

The performance of the predictive models for ECD was assessed using Mean Squared Error (MSE), Mean Absolute Error (MAE), Root Mean Squared Error (RMSE), and the coefficient of determination (R^2). These evaluation metrics guided the selection of optimal hyperparameter values for each algorithm, following the experimental framework described in Table 2. Among the SVM variants, the model utilizing a linear kernel with a 'scale' kernel coefficient exhibited the best performance, achieving an R^2 of 0.9822. For the RF model, the configuration with 60 decision trees yielded the most accurate results, with an R^2 of 0.9851. For the remaining three models, the ANN model also demonstrated high predictive accuracy, achieving an R^2 value of 0.9816. Similarly, the GB model produced reliable results with an R^2 of 0.9406. The XGBoost model likewise exhibited strong performance, attaining an R^2 value of 0.9911.

3.2 Results of ECD model predictions from testing data

Table 3 shows that the RF model with 60 estimators demonstrated the highest accuracy among the five evaluated algorithms when applied to the testing dataset. It achieved the lowest MSE (0.000998), MAE (0.0032), and RMSE (0.0316), along with the highest R^2 value of 0.992888. This superior performance is further supported by the comparison of ECD prediction results across models for both training and testing datasets, as shown in Table 4. Consequently, the RF model was identified as the most accurate and efficient method for predicting ECD values. Closely following in performance is the SVM model with a linear kernel, which yielded MSE, MAE, RMSE, and R^2 of 0.0024, 0.0414, 0.0490, and 0.9855, respectively. The similarity in R^2 values between the training and testing results indicates that the model generalizes well and is unlikely to be overfitted.

As illustrated in Figure 3, the distribution plot of the test dataset shows that most predicted ECD values are within less than or equal to 2 SG (red line), forming a roughly bimodal pattern. The distribution is slightly right-skewed, indicating a few higher ECD values above 1.6 SG. The dataset has a moderate spread, suggesting some variability in the drilling conditions. A few isolated high-value points may represent abnormal circulation events or sensor noise. Comparing the distribution of actual value with the predicted value (blue line) of each model, both show a similar pattern and closely aligned central tendencies, indicating that the model captures the main behavior of the data. The predicted distributions produced by the SVM and GB models appear to be slightly wider than the actual distribution, indicating a tendency to overestimate values near the central range. In contrast, the ANN model provides a more accurate estimation of ECD compared with SVM and GB; however, its predicted distribution becomes slightly narrower with minor bias in the tails. Notably, the RF model demonstrates the closest agreement with the actual distribution, with its predicted curve nearly overlapping the actual values across the entire ECD range.

According to the results of the algorithm comparative study, the RF model achieved the highest performance among the four algorithms evaluated. These results are consistent with those of prior research by Alsaihati et al., 2021, who also identified RF as the most accurate model for ECD prediction. Notably, the RMSE in this study (0.03) is significantly lower than the 0.42 reported by Alsaihati et al., 2021, demonstrating a substantial enhancement in predictive accuracy. Although the SVM model using a linear kernel also demonstrated strong predictive performance (R^2 = 0.9855), which is in line with the findings from Ahmadi et al., 2016 and Alsaihati et al., 2021 which R^2 is 0.99, that study was limited by a smaller variable set (pore pressure, temperature, and clay density) and lacked detailed information on dataset size and preprocessing steps. In contrast, the present study employed a larger, more diverse dataset aligned with theoretical ECD modeling practices (Raabe and Jortner, 2021), contributing to its robust and generalizable results. Nevertheless, XGBoost is moreover more accurate than the ANN model. These results are consistent with those of previous studies by Abdelgawad et al., 2019, H. Alkinani et al., 2019, and Gamal et al., 2021a.

Table 3 Comparison of ECD prediction performance among 5 algorithms for the testing dataset

Algorithms	Comparison of Models Performance			
	MSE	MAE	RMSE	R^2
SVM	0.0024	0.0414	0.0490	0.9855
RF	0.0010	0.0031	0.0316	0.9929
ANN	0.0048	0.0158	0.0696	0.9602
GB	0.0084	0.0179	0.0915	0.9403
XGBoost	0.0037	0.0050	0.0611	0.9734

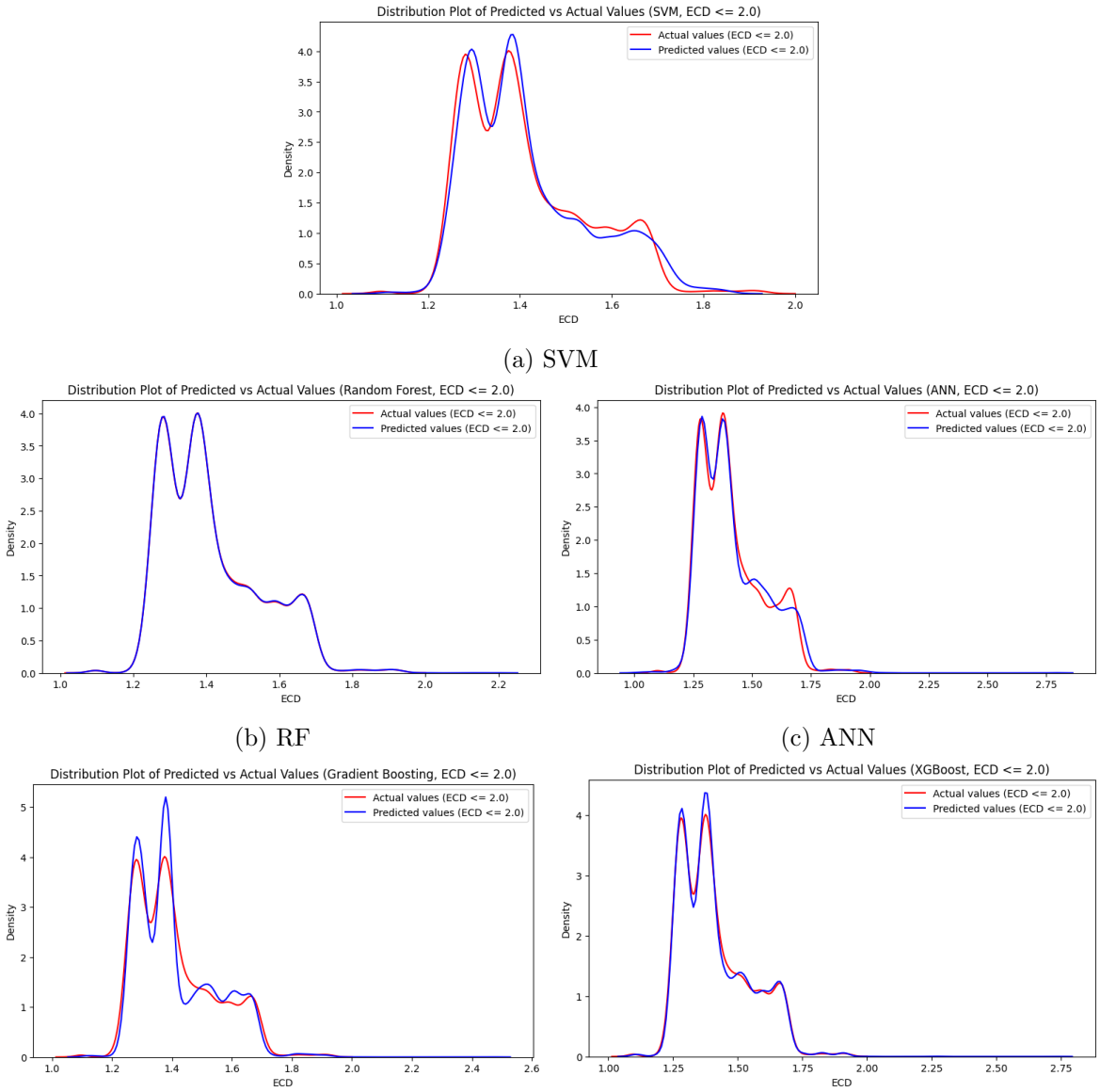

(a) SVM

(b) RF

(c) ANN

(d) GB

(e) XGBoost

Figure 3 Comparison of the distribution between the actual and predicted ECD values by 5 algorithms

Table 4 Comparison of ECD prediction performance among each model using the training and testing datasets

Algorithms	R^2	
	Train	Test
SVM	0.982162	0.985469
RF	0.985139	0.992888
ANN	0.981568	0.960218
GB	0.940570	0.940343
XGBoost	0.991051	0.973387

The superior performance of the RF model highlights its suitability for real-time ECD prediction, where high accuracy and robustness are essential. The ensemble-based structure of RF enables the effective learning of complex and nonlinear relationships among drilling and mud parameters, which are often inadequately captured by traditional modeling approaches. Moreover, the robustness of RF to noise and outliers is particularly advantageous for real-time

sensor data, which are inherently subject to measurement uncertainty. The ability of RF to handle high-dimensional input spaces, incorporating both surface and downhole measurements, further enhances its applicability in real-time drilling operations. These findings support the argument that simpler yet efficient ensemble-based AI models may offer a favorable balance between predictive accuracy and computational efficiency for real-time applications consistent with the observations of (Dabiri et al., 2025)

Feature importance analysis (Figure 4) was performed using the RandomForest model, which achieved the best predictive accuracy among all tested algorithms. The results show that Downhole Annulus Pressure (DHAP) is the most influential variable (0.7792) in predicting ECD, reflecting its direct impact on annular pressure during circulation. Annular pressure loss and hole inclination also exhibit high importance scores, indicating their strong contribution to variations in ECD under different wellbore annulus pressure. In addition, Mud Density (Mud_Wt_Out) is the second most important parameter (0.1160). Conversely, parameters such as Downhole Annulus Temperature (DHAT) and Depth (DEPT) demonstrate comparatively lower importance, suggesting a limited effect on ECD prediction within the operating range of the dataset. These results are consistent with drilling hydraulics theory, where fluid flow and well geometry predominantly determine the equivalent circulating density.

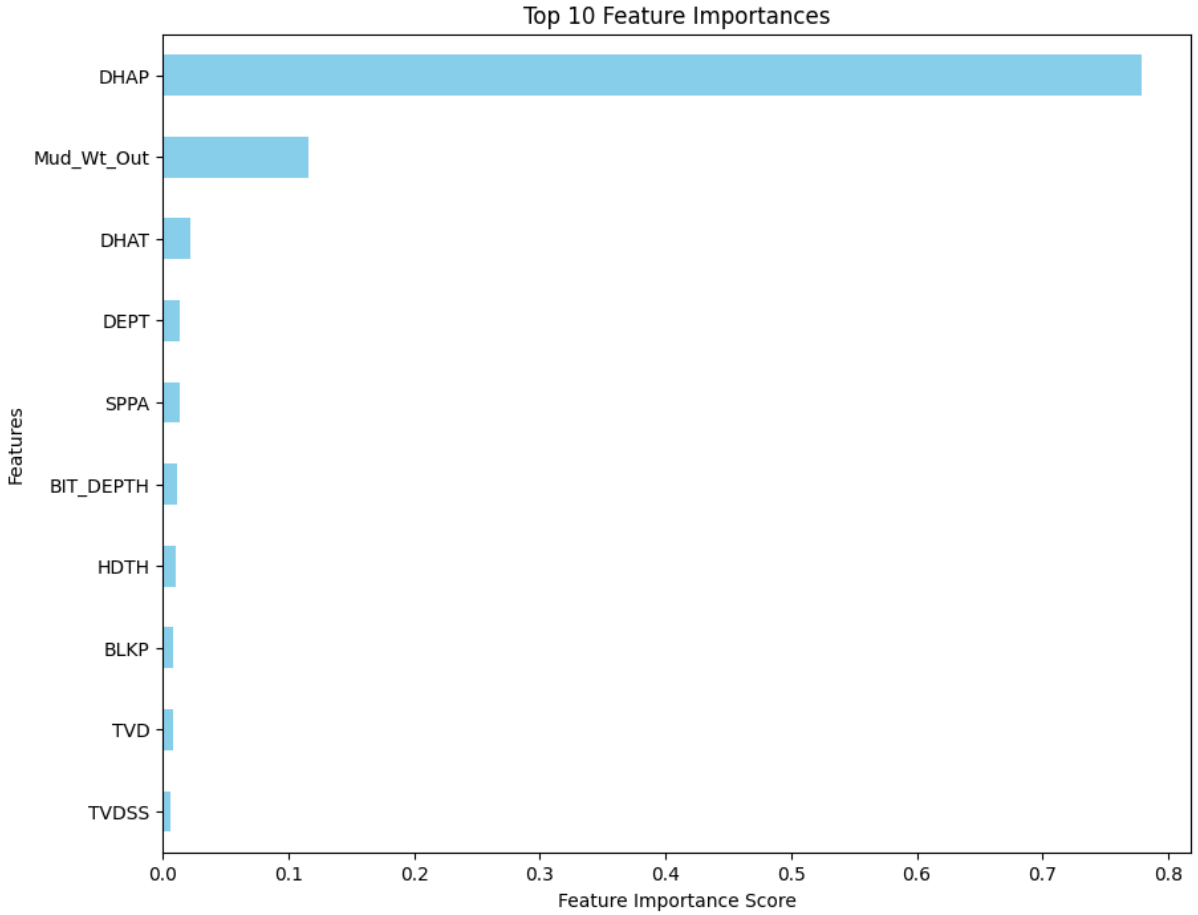

Figure 4 Top 10 importance features for the RF model

Pre-drill Equivalent Circulating Density (ECD) estimation remains a critical area that warrants further investigation and development (H. H. Alkinani et al., 2020). A review of the existing literature further indicates that persistent research gaps remain in the application of machine learning (ML) techniques to drilling operations (Osarogiagbon et al., 2021; Waqar et al., 2023). These gaps can be summarized as follows: (1) Real-time, field-scale validation of ML models is still limited, raising concerns regarding their performance under actual operational conditions (Osarogiagbon et al., 2021; Løken et al., 2021); (2) many ML models are developed and de-

ployed with insufficient emphasis on interpretability, which hinders their practical adoption in operational settings (Olukoga and Feng, 2021; Waqar et al., 2023); and (3) existing studies lack sufficient integration of geographically diverse data and varied operational environments, leaving many regions and drilling conditions underrepresented in current ML-based investigations (Waqar et al., 2023).

For future research, the development of new techniques to develop the predictive models using datasets from a broader range of drilling sites across the Gulf of Thailand is recommended. Such an approach would increase confidence in the generalizability and robustness of the models under varying geological and operational conditions. If performance limitations are identified, the models can be further enhanced by incorporating data from more diverse drilling environments to improve predictive accuracy. These expanded studies would not only deepen the understanding of model behavior across different scenarios but also facilitate their application in a wider array of drilling operations. This could ultimately contribute to increased operational efficiency by reducing drilling-related risks and hazards. Moreover, further development of the models for ECD prediction anomaly analysis as the study of El-Hadad et al., 2022 or estimating the abnormal events occurring in the wellbore as the study of Nugroho et al., 2023 with real-time environmental and drilling parameters.

4. Conclusions

In conclusion, the RF model stands out as the most accurate, efficient, and robust approach for predicting ECD in the 6.125-inch production section in the Gulf of Thailand. Its simplicity, low risk of overfitting, robustness to noise, ability to capture nonlinear relationships, and compatibility with standard MWD and LWD data make it particularly suitable for real-time applications. The implementation of such real-time predictive capabilities during drilling operations could significantly mitigate risks and reduce dependence on physical measurement tools. For example, replacing PWD tools with predictive models could lead to substantial cost savings—estimated at 1.5–2.0% of the THB per well and up to 48 million THB per project thereby enhancing the overall economic efficiency of drilling operations. In this context, cost reduction plays a crucial role in optimizing drilling workflows and improving decision making in real time. This approach further enhances workflow reliability and strengthens confidence in operational safety. With appropriate adjustments to handle live data input, this model holds strong potential for deployment in dynamic drilling environments to support real-time ECD monitoring and decision making. In this study, an 80:20 train-test split was employed instead of k-fold cross-validation because of the computational efficiency when working with large datasets. The results showed comparable R^2 values between the training and testing sets, indicating a low risk of overfitting. Therefore, the use of an 80:20 split is appropriate and effective for this application. Nevertheless, when applying the machine learning models to different datasets in the future, other data splitting methods, such as cross validation, may be employed to confirm and demonstrate model robustness.

Acknowledgements

The authors would like to express their sincere gratitude to the Case Study Company, the drilling process control personnel, the measurement and data collection teams during drilling operations, and all staff at the drilling site for their valuable cooperation and assistance in effectively gathering the various variable data from the drilling process.

Author Contributions

K. L. conceptualized the thesis study, built the model, and performed data analysis and interpretation. S. S. prepared the data and built the ML model, K. S. wrote the manuscript, interpreted the results, and reviewed the manuscript. K.B. contributed to conceptualization, results interpretation, and review of the manuscript.

References

Abdelaal, A., Elkatatny, S., Gamal, H., & Ziadat, W. (2023). Drilling data-based approach for equivalent circulation density prediction while drilling. *ARMA US Rock Mechanics/Geomechanics Symposium*, ARMA–2023. https://doi.org/10.56952/ARMA-2023-0722

Abdelgawad, K. Z., Elzenary, M., Elkatatny, S., Mahmoud, M., Abdulraheem, A., & Patil, S. (2019). New approach to evaluate the equivalent circulating density (ecd) using artificial intelligence techniques. *Journal of Petroleum Exploration and Production Technology*, *9*(2), 1569–1578. https://doi.org/10.1007/s13202-018-0572-y

Ahmadi, M. A. (2016). Toward reliable model for prediction of drilling fluid density at wellbore conditions: A lssvm model. *Neurocomputing*, *211*, 143–149. https://doi.org/10.1016/j.neucom.2016.01.106

Ahmadi, M. A., Shadizadeh, S. R., Shah, K., & Bahadori, A. (2016). An accurate model to predict drilling fluid density at wellbore conditions. *Egyptian Journal of Petroleum*, *27*(1), 1–10. https://doi.org/10.1016/j.ejpe.2016.12.002

Al-Hameedi, A. T., Dunn-Norman, S., Alkinani, H. H., Flori, R. E., & Hilgedick, S. A. (2017). Limiting drilling parameters to control mud losses in the dammam formation, south rumaila field, iraq. *ARMA US Rock Mechanics/Geomechanics Symposium*, ARMA–2017. https://doi.org/https://doi.org/10.1016/j.ejpe.2019.12.003

Ali, J. K. (1994). Neural networks: A new tool for the petroleum industry? *SPE European Petroleum Computer Conference*, SPE–27561. https://doi.org/10.2118/27561-MS

Alkinani, H., Al-Hameedi, A. T., Dunn-Norman, S., & Al-Alwani, M. A. (2019). Data-driven neural network model to predict equivalent circulation density ecd. *SPE Gas & Oil Technology Showcase and Conference*. https://doi.org/10.2118/198612-MS

Alkinani, H. H., Al-Hameedi, A. T. T., Dunn-Norman, S., & Lian, D. (2020). Application of artificial neural networks in the drilling processes: Can equivalent circulation density be estimated prior to drilling? *Egyptian Journal of Petroleum*, *29*(2), 121–126. https://doi.org/10.1016/j.ejpe.2019.12.003

Alsaihati, A., Elkatatny, S., & Abdulraheem, A. (2021). Real-time prediction of equivalent circulation density for horizontal wells using intelligent machines. *ACS Omega*, *6*(1), 934–942. https://doi.org/10.1021/acsomega.0c05570

Amado, L. (2013). *Reservoir exploration and appraisal*. Gulf Professional Publishing.

Awad, M., & Khanna, R. (2015). Support vector regression. In *Efficient learning machines* (pp. 67–80). Apress Open. https://doi.org/10.1007/978-1-4302-5990-9_4

Bahaloo, S., Mehrizadeh, M., & Najafi-Marghmaleki, A. (2023). A review of application of artificial intelligence techniques in petroleum operations. *Petroleum Research*, *8*(2), 167–182. https://doi.org/10.1016/j.ptlrs.2022.07.002

Cutler, A., Cutler, D. R., & Stevens, J. R. (2012). Random forests. In *Ensemble machine learning: Methods and applications* (pp. 157–175). Springer. https://doi.org/10.1007/978-1-4419-9326-7

Dabiri, M. S., Haji-Hashemi, R., Hemmati-Sarapardeh, A., Zabihi, R., Mohammadi, M. R., Schaffie, M., & Ostadhassan, M. (2025). Artificial intelligence approaches to modeling equivalent circulating density for improved drilling mud management. *ACS Omega*, *10*(18), 19157–19174. https://doi.org/10.1021/acsomega.5c02050

El-Hadad, R., Tan, Y.-F., & Tan, W.-N. (2022). Anomaly prediction in electricity consumption using a combination of machine learning techniques. *International Journal of Technology*, *13*(6), 1317–1325. https://doi.org/https://doi.org/10.14716/ijtech.v13i6.5931

Gallo, C. (2015). Artificial neural networks tutorial. In *Encyclopedia of information science and technology, third edition* (pp. 6369–6378). IGI Global Scientific Publishing. https://doi.org/10.4018/978-1-4666-5888-2.ch626

Gamal, H., Abdelaal, A., & Elkatatny, S. (2021a). Intelligent prediction of the equivalent circulating density from surface data sensors during drilling by employing machine learning techniques. https://doi.org/10.21203/rs.3.rs-154257/v1

Gamal, H., Abdelaal, A., & Elkatatny, S. (2021b). Machine learning models for equivalent circulating density prediction from drilling data. *ACS Omega*, *6*(36), 27430–27442. https://doi.org/10.1021/acsomega.1c04363

Goyal, P. (2021). Gradient boosting algorithm: A complete guide for beginners [Analytics Vidhya].

Hadi, A. B. (2023). Drilling technology cost. In *Tight oil reservoirs characterization, modeling, and field development* (pp. 315–331, Vol. 1). Gulf Professional Publishing. https://doi.org/10.1016/B978-0-12-820269-2.00008-1

Hegde, C., & Gray, K. E. (2017). Use of machine learning and data analytics to increase drilling efficiency for nearby wells. *Journal of Natural Gas Science and Engineering*, *40*, 327–335. https://doi.org/10.1016/j.jngse.2017.02.019

International Association of Oil & Gas Producers. (2023). Drilling methods.

Løken, E. A., Løkkevik, J., & Sui, D. (2021). Testing machine learning algorithms for drilling incidents detection on a pilot small-scale drilling rig. *Journal of Energy Resources Technology*, *143*(12), 124501. https://doi.org/10.1115/1.4052284

Mitchell, R. F., & Miska, S. Z. (Eds.). (2011). *Fundamentals of drilling engineering* (Vol. 2). Society of Petroleum Engineers. https://doi.org/10.2118/9781555632076

Noorsaman, A., Amrializzia, D., Zulfikri, H., Revitasari, R., & Isambert, A. (2023). Machine learning algorithms for failure prediction model and operational reliability of onshore gas transmission pipelines. *International Journal of Technology*, *14*(3), 680–689. https://doi.org/https://doi.org/10.14716/ijtech.v14i3.6287

Nugroho, H. A., Subiantoro, A., & Kusumoputro, B. (2023). Performance analysis of ensemble deep learning narx system for estimating the earthquake occurrences in the subduction zone of java island. *International Journal of Technology*, *14*(7), 1517–1526. https://doi.org/https://doi.org/10.14716/ijtech.v14i7.6702

Okonkwo, S. I. F., & Joel, O. F. (2023). Modeling the effects of temperature and pressure on equivalent circulating density (ecd) during drilling operations using artificial neural networks. *Journal of Engineering Research and Reports*. https://doi.org/10.9734/jerr/2023/v25i9982

Olukoga, T. A., & Feng, Y. (2021). Practical machine-learning applications in well-drilling operations. *SPE Drilling & Completion*, *36*(04), 849–867. https://doi.org/10.1115/1.4052284

Osarogiagbon, A. U., Khan, F., Venkatesan, R., & Gillard, P. (2021). Review and analysis of supervised machine learning algorithms for hazardous events in drilling operations. *Process Safety and Environmental Protection*, *147*, 367–384. https://doi.org/10.2118/205480-PA

Pedregosa, F., Varoquaux, G., Gramfort, A., Michel, V., Thirion, B., Grisel, O., Blondel, M., Prettenhofer, P., Weiss, R., Dubourg, V., Vanderplas, J., Passos, A., Cournapeau, D., Brucher, M., Perrot, M., & Duchesnay, E. (2011). Machine learning in python. *Journal of Machine Learning Research*, *12*, 2825–2830.

Raabe, G., & Jortner, S. (2021). Chapter one - well control discussion and theories. In *Universal well control* (1st). Gulf Professional Publishing. https://doi.org/10.1016/C2020-0-03930-7

Rahmati, A. S., & Tatar, A. (2019). Application of radial basis function (rbf) neural networks to estimate oil field drilling fluid density at elevated pressures and temperatures. *Oil & Gas Science and Technology–Revue d'IFP Energies nouvelles*, *74*, 50. https://doi.org/10.2516/ogst/2019021

Roy, V., Pandey, A., Saxena, A., & Sharma, S. (2022). Assessment of machine learning techniques for real-time prediction of equivalent circulating density. *Offshore Technology Conference Asia*, D041S039R006. https://doi.org/10.4043/31523-MS

Saasen, A. (2013). Annular frictional pressure losses during drilling: The effect of drillstring rotation. *International Conference on Offshore Mechanics and Arctic Engineering*, V006T11A001. https://doi.org/10.1115/OMAE2013-10185

Sun, Z., Zhang, C., & Zhu, J. (2020). Numerical studies of the effects of fluid density on the flow structures in circulating fluidized beds. *Proceedings of the Canadian Society for Mechanical Engineering Annual Conference*, 1–10. https://doi.org/10.32393/csme.2020.65

Waqar, A., Othman, I., Shafiq, N., & Mansoor, M. S. (2023). Applications of ai in oil and gas projects towards sustainable development: A systematic literature review. *Artificial Intelligence Review*, *56*(11), 12771–12798. https://doi.org/10.1007/s10462-023-10467-7